Performance investigation of direct-expansion solar medium- and high-temperature heat pump systems with vacuum tubes

Qing Xu[a], Xiaohui Yu[a,*], Qinqin Kong[a], Shihao Li[a]

[a]School of Energy and Environment Engineering, Hebei University of Technology, Tianjin 300401, PR China

Abstract

With the continuous growth of global energy demand and increasing emphasis on environmental protection, solar energy has garnered significant attention due to its clean and renewable characteristics. Solar thermal utilization technology has consequently emerged as a key research focus in sustainable energy conversion. The direct-expansion solar-assisted medium- and high-temperature heat pump (DX-SAMHTHP) system integrates the advantages of solar thermal utilization and medium-/high-temperature heat pump technology. It efficiently upgrades low-grade solar thermal energy into high-grade heat energy, suitable for industrial heating, domestic hot water, and other fields. This paper presents the design and construction of an experimental bench for a vacuum tube-based DX-SAMHTHP system in a laboratory setting. This experiment adopted a configuration with two vacuum tube collector-evaporators connected in series, using R1233zd(e) as the refrigerant. The thermal output temperature was set at 70-85 °C, and the system was experimentally investigated under multiple operating conditions to analyze its specific effects on energy performance. The effects of solar irradiance (564.9-1123.6 $W \cdot m^{-2}$), heat output temperature (70-85 °C), ambient temperature (28.31-32.15 °C), and collector area (1.5 m^2, 3.0 m^2) on the system were investigated using the coefficient of performance (COP) and collector efficiency as performance indicators. The results demonstrate that the proposed system can stably supply heat at 70–85 °C with a COP of up to 6.11, validating its technical feasibility. A key finding is the inherent trade-off between system COP and collector efficiency when increasing the collector area or solar irradiance. This work provides a foundational experimental study for the development of efficient solar-assisted medium-to-high temperature heat pumps.

Keywords: Direct-expansion solar-assisted heat pump, Moderate and high temperature heat pump, Vacuum tube collector-evaporator, Energy performance;

1. Introduction

In recent years, the issue of global climate change has become increasingly severe, with frequent occurrences of extreme weather events significantly impacting human life. Consequently, the transformation of the energy structure system has become an urgent priority. Gradually reducing dependence on fossil fuels and increasing the use of renewable energy sources has become a global consensus. Solar energy, as a renewable resource with abundant reserves, clean and environmentally friendly characteristics, widespread distribution, and enormous development potential [1-2], not only provides a clean, renewable energy supply to meet global energy demands but also helps reduce greenhouse gas emissions and fossil fuel consumption. It has gained extensive application worldwide [3].

In 1955, Sporn and Ambrose first explicitly proposed the concept of a direct expansion solar air heat pump (DX-SAHP) system. Compared to conventional heat pumps, it offers superior thermodynamic performance, a smaller footprint, lower system costs, and a longer service life [4-6]. Due to these unique advantages, DX-SAHP technology has garnered significant attention within the academic community and has been widely

* Corresponding author. Tel.: +8615102282362
E-mail address: 2018133@hebut.edu.cn (Xiaohui Yu)

applied in fields such as water heating, solar drying, air conditioning, and cold storage [7-8]. To enhance utilization rates, reduce operating costs, and fully leverage existing solar energy, researchers have conducted extensive studies on DX-SAHP systems. These investigations mainly focused on collector-evaporator design [8] and system integration and optimization [9].

Recent advancements in DX-SAHP systems have explored advanced collector-evaporator configurations, including evacuated tubes, compound parabolic concentrators (CPC), photovoltaic/thermal (PV/T) hybrids, and micro-channel designs, aiming to improve energy capture and conversion efficiency [10-12]. However, current research on the thermal performance of DX-SAMHTHP systems remains limited, hindering deeper understanding of these systems and constraining their further development and practical application. Moreover, there is an urgent need to explore innovative configurations of direct-expansion solar-assisted heat pump systems, particularly those employing solar collector-evaporators. This approach aims to achieve higher performance, enhanced reliability, and lower energy consumption while consistently delivering medium-to-high temperature heat above 70 °C.

To address this research gap, this study presents what is, to the best of the authors' knowledge, the first experimental investigation of a direct-expansion solar-assisted medium-to-high temperature heat pump system that utilizes evacuated tube collectors and the refrigerant R1233zd(E), operating stably within the 70–85 °C range. By integrating vacuum tube collection, direct expansion solar utilization, and medium-to-high temperature heat pump technologies, this system enhances overall performance while expanding the application potential of medium-to-high temperature heat pump technology. The objective of this study is to quantitatively evaluate the performance advantages of the proposed vacuum tube direct expansion solar medium-to-high temperature heat pump system and conduct an in-depth analysis of its thermodynamic characteristics to enhance system performance and reduce operating costs. An experimental platform for a vacuum-tube direct-expansion solar medium-to-high-temperature heat pump system was designed and constructed, with an in-depth analysis of its thermal performance. When the thermal output temperature was set within the range of 70°C to 85°C, the system's thermal performance was primarily evaluated based on two metrics: the COP and the collector efficiency. The effects of solar irradiance, thermal output temperature, ambient temperature, and collector area on the system's thermal performance were compared and studied.

The present study has certain limitations. Experimental conditions were confined to a specific location, with ambient temperatures (≈28–32 °C) and solar irradiance (≈565–1125 $W \cdot m^{-2}$) limited to favorable daytime conditions. System performance under low/cold temperatures, nighttime operation, and seasonal variations was not investigated. Additionally, the setup featured fixed component sizes without thermal energy storage or auxiliary heating-critical for continuous heat supply during low/no solar availability. Future work will focus on: long-term seasonal testing (including winter/transitional seasons) to cover wider temperature and solar input ranges; integrating thermal energy storage and auxiliary heat sources for 24/7 operation; developing dynamic simulation models for system optimization, scaling, and control strategy exploration; and conducting comprehensive techno-economic assessments to evaluate commercial viability across different regions.

2. Methods

2.1. System description

The schematic and external configuration of the vacuum-tube-based direct-expansion solar medium-to-high-temperature heat pump system are shown in Figure 1. As shown in Figure 1, the system employing a vacuum tube collector evaporator comprises two circuits: the red line represents the refrigerant circuit, while the blue line denotes the heat output circuit. The refrigerant circuit primarily consists of an electronic expansion valve, compressor, vacuum tube heat-collecting evaporator, and immersion condenser. This experiment employed two sets of vacuum tube collector evaporators connected in series. The heat output circuit primarily consists of the water pump, water tank, and radiator. The parameters of each component in the refrigerant circuit and heat output circuit are shown in Table 1. This system selected R1233zd(e) as the refrigerant.

Table 1 Parameters of refrigerant and heat output circuit components

Equipment	Type	Specification
Vacuum tube solar collector-evaporator	ZKJRQ10	Collective evaporator area: 1.5 m^2 Vacuum tube outer diameter: 100 mm Effective tube length: 1500 mm Refrigerant inner tube runner: 10 mm

		Effective length of inner tube: 1350 mm Refrigerant outer tube runner: 19 mm Effective length of outer tube: 1480 mm Rated heat transfer capacity: 4 kW
Compressor	PH161X8ECT-KCEF1	Type: Hermetic Rotor Compressor Rated power: 1 HP Rated voltage: 220-240 V
Immersion condenser	ELN96H	Rated heat transfer capacity: 3 kW
Expansion valve	DPF(Q) 1.8C	Maximum circulating refrigerant flow: 0.1 m^3/h Adjustment range: 0-500 steps
Gas-liquid separator	PKQ-204	Available Capacity: 1.5 L Design Pressure: 3 MPa
Pump	25SGR3-15	Rated power: 370 W
Water tank	YC30	Available capacity: 35 L

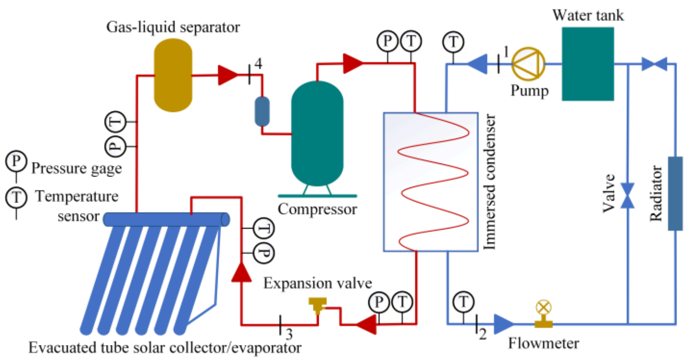

Figure 1. Experimental system diagram of the DX-SAMHTHP system experimental apparatus for vacuum tubes

The layout of measurement points for key parameters (pressure, power, temperature, irradiance, and flow rate) is illustrated in Fig. 1 (a), with detailed instrument specifications provided in Table 2. Test data were recorded every 10-second interval and transmitted via a paperless recorder.

Table 2 Detailed parameters of measurement

Equipment	Type	Measurement range	Accuracy
Pressure gage	WT-3.8	-0.1-3.8 (MPa)	±1.6 % FS
	WT-1.8	-0.1-1.8 (MPa)	±1.6 % FS
Power measuring instrument	RK9800N	0-2400 (W)	±0.4 % FS
Temperature sensor	PT100	-50-250 (°C)	±0.15+0.002*|t| (°C)
Solar radiation meter	TBQ-2	0-2000 (W/m2)	±5 % FS
Flowmeter	SGLWGY-G-D20	0.45-9.00 (m3/h)	±0.5 % FS

2.2. Data acquisition

For simplicity, the following assumptions were made in the performance analysis:

(1) All system components operate under steady-state conditions with stable flow rates;

(2) The heat released by the condenser equals the heat absorbed by the circulating water;

(3) Resistance and heat losses within the collector evaporator, condenser, and connecting pipes are neglected.

COP is a critical metric for evaluating energy conversion efficiency. The collector efficiency metric assesses how effectively a vacuum tube collector evaporator converts received solar radiation into usable thermal energy. Therefore, COP and collector efficiency (η_{col}) are selected as indicators for evaluating the overall system performance.

$$COP = \frac{Q_w}{W_{com}} = \frac{c_w m_w (T_2 - T_1)}{W_{com}} \tag{1}$$

$$\eta_{col} = \frac{Q_{col}}{IA_{col}} = \frac{m_r (h_4 - h_3)}{IA_{col}} \tag{2}$$

Where Q_w is the heating capacity, W; W_{com} denotes compressor input power, W; c_w is the specific heat capacity of water, J/(kg·°C); m_w is the mass flow rate of water, kg/s; T is the temperature, °C; Subscripts 1 and 2 denote the inlet and outlet of the condenser circulating water, respectively; m_r is the refrigerant mass flow rate, kg/s; Subscripts 4, 3 are the outlet and inlet of the solar collector-evaporator, respectively; A_{col} is the effective heat collection area of the vacuum tube evaporator, m^2; I is the solar radiation intensity, W/m^2; Q_{col} is refrigerant's effective heat absorption in the collector evaporator, W.

2.3. Uncertainty analysis

The uncertainty of indirect parameters, determined from mathematical models and experimental data, can be obtained by the uncertainty propagation method. This method assumes that the indirect parameter R is determined by several directly measured parameters $X_1, X_2, \ldots, X_n$ and that these quantities are uncorrelated with one another. The relative compound uncertainty is:

$$u_{rel} = \frac{u(R)}{R} = \frac{\sqrt{\sum_{i=1}^{n} \left(\frac{\partial R}{\partial X_i} \delta X_i\right)^2}}{f(X_1, X_2, \ldots, X_n)} \tag{3}$$

The maximum relative uncertainty of the COP, heat collector efficiency and heat capacity for this proposed system was 2.43%, 5.73% and 2.12%, respectively.

3. Results and discussion

3.1. Effect of Solar irradiation on system efficiency

The experiment was conducted under the following conditions: ambient temperature (T_a) of 29.6 °C, wind speed of approximately 0.03 m·s^{-1}, heat output temperature (T_{out}) of 80 °C, and solar irradiance (I) ranging from 564.9 to 1123.6 W·m^{-2}. Figure 2 shows the variation of compressor power consumption (W_{com}), system heating capacity (Q_w), COP, and collector efficiency (η_{col}) with I. The figure clearly indicates that as I increases, W_{com}, Q_w, and COP all gradually rise, while η_{col} exhibits a linear decreasing trend. As I increases from 564.9 W·m^{-2} to 1123.6 W·m^{-2}, W_{com} rises from 154.48 W to 208.34 W, exhibiting an approximately linear growth relationship. Concurrently, the Q_w exhibits a more pronounced increase, rising from approximately 801.76 W to nearly 1185.45 W. The system's COP also improved by 9.6%, rising from 5.19 to 5.69. However, the η_{col} decreased from 0.96 to 0.70, representing a decline of 27.1%. This reflects that under high irradiation conditions, the heat loss of the collector relatively increased, with the heat absorption gain failing to offset the radiation loss, leading to a decrease in efficiency. Despite the reduced η_{col}, the high irradiation conditions still caused the system evaporation temperature to rise, thereby enhancing the COP. This demonstrates that the system maintains good thermal conversion performance under strong solar radiation.

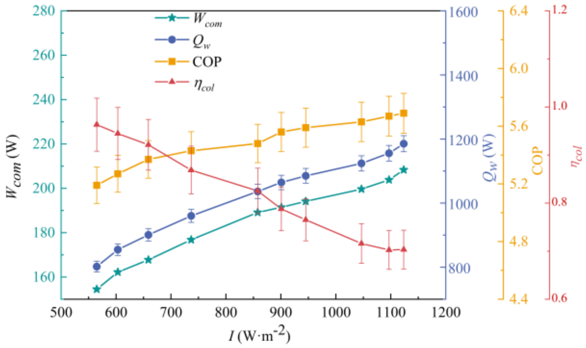

Figure 2. Changes of the compressor power consumption, heating power, COP, and heat collection efficiency with solar radiation intensity

3.2. Effect of heat output temperature on energy efficiency

This study evaluated the system's performance at T_{out} of 70 °C, 75 °C, 80 °C, and 85 °C. Superheat was maintained at 6±1 °C, and T_a was controlled around 29 °C. Figure 3 shows the COP and η_{col} of different T_{out} systems at I levels ranging from 700 to 1000 W·m^{-2}. As shown in the figure, when the heat output temperature increases, the system's COP value exhibits a downward trend, while the η_{col} shows an upward trend. When I ranges from 700 to 1000 W·m^{-2}, the average system COP value is 5.70 at a T_{out} of 70°C. At T_{out} of 75°C, 80°C, and 85°C, the average system COP values are 5.62, 5.51, and 5.46, respectively, representing decreases of 1.41%, 3.36%, and 4.12%, respectively. This is because, as the T_{out} rises, the compressor requires a higher heating pressure ratio, leading to increased energy consumption. Meanwhile, the amount of heat absorbed from the environment by the system increases only marginally, resulting in a decline in overall COP. Compared to the average η_{col} of 0.77 at 70 °C, the η_{col} at 75 °C, 80 °C, and 85 °C increased by 4.25%, 7.89%, and 11.28%, respectively. This is because when the system operates under high pressure ratio conditions, the operating temperature of the collector is forced to decrease, thereby correspondingly reducing the heat dissipation loss from the collector to the environment and leading to an increase in the η_{col}.

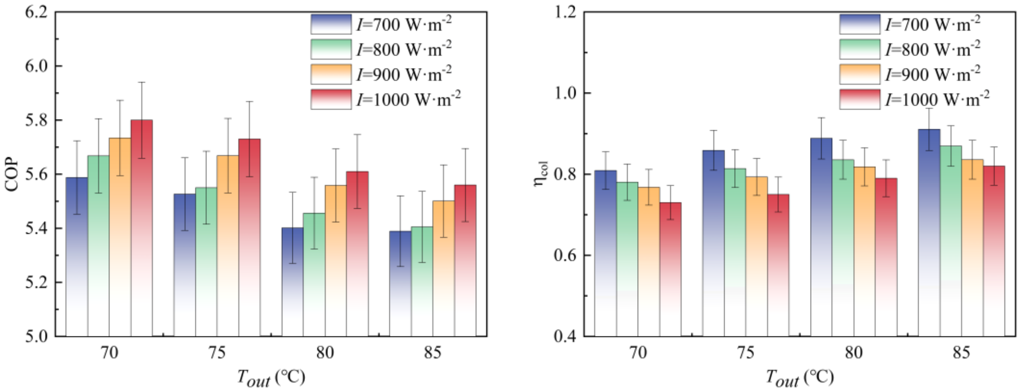

(a) (b)

Figure 3. Changes of the (a) COP and (b) heat collection efficiency with heat output temperature

3.3. Effect of ambient temperature on energy efficiency

Based on I of 1040±15 W·m^{-2} and wind speed of 1.5±0.3 m·s^{-1}, the impact of T_a variations within the range of 28.31–32.15 °C on system performance is illustrated in the figure below. Figure 4 illustrates the changes in W_{com}, Q_w, COP, and η_{col} as T_a increases. Q_w, COP, and η_{col} all gradually increase with rising T_a. Compressor power consumption remains relatively stable overall. When T_a ranges from 27.76 to 34.52 °C, the corresponding COP varies between 5.60 and 5.87, while η_{col} rises from 0.71 to 0.76. In summary, system performance improves with rising T_a This occurs because higher T_a reduces the temperature difference between the collector evaporator and the environment, decreasing heat transfer losses and thereby enhancing η_{col}. Compressor suction pressure increases accordingly, while discharge pressure remains relatively stable, leading to an increase in the COP value.

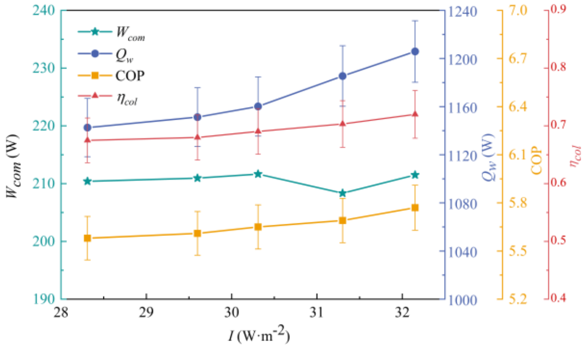

Figure 4. Changes of the compressor power consumption, heating power, COP, and heat collection efficiency with ambient temperature

3.4. Effect of collector area on energy efficiency

At an T_a of 29.6±1°C, wind speed of approximately 0.5±0.1 m/s, and I within the range of 700–1000 W·m^{-2}, the influence of collector area on system thermal performance was investigated for collector areas of 1.5 m^2 and 3.0 m^2. As shown in Figure 5, with a collector area of 3 m^2, the COP increased from 5.73 to 6.11 and the η_{col} decreased from 0.76 to 0.69, respectively. Compared to the heat pump system with a 1.5 m^2 collector area, the average COP increased by 7.04%, while the average η_{col} decreased by 12.33%. This trade-off is attributed to the enlarged collector area. The increased solar absorption raises the refrigerant evaporation temperature and compressor suction pressure, thereby reducing the compressor pressure ratio and its power consumption, which improves the COP. Concurrently, the higher refrigerant temperature within the collector, especially when it exceeds T_a, intensifies heat loss to the environment, resulting in a lower η_{col}.

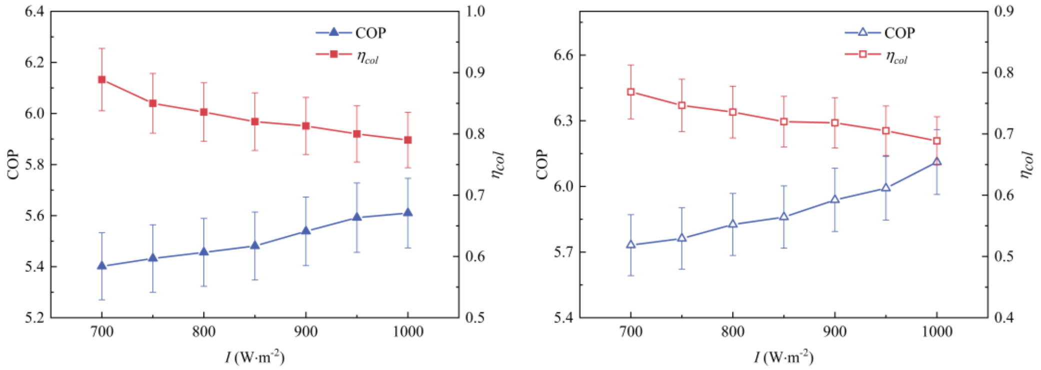

(a) Vacuum tube collector-evaporator collector area: 1.5 m^2 (b) Vacuum tube collector-evaporator collector area: 3.0 m^2

Figure 5. Changes of the COP and heat collection efficiency in different vacuum tube collector-evaporator areas

4. Conclusions

This work establishes and tests a vacuum-tube-based direct-expansion solar-assisted medium-to-high temperature heat pump (DX-SAMHTHP) system capable of stable 70–85 °C heat output. The system exhibits high performance (COP up to 5.7–6.1) across varied conditions, marking the first experimental proof of concept for a DX solar heat pump using vacuum tube collectors and R1233zd(E) refrigerant at these temperatures. A key finding is the performance trade-off: larger collector area or higher irradiance boosts system COP by raising evaporation temperature but reduces collector efficiency due to increased heat loss. This underscores a pivotal design principle: optimizing for overall system COP is paramount, not just collector efficiency. The study demonstrates a viable solar-thermal solution for industrial heating (e.g., food processing, textiles). Future efforts should target long-term seasonal testing, multi-climate validation, and model development for system scale-up and control optimization.

The present study is subject to certain limitations. The experimental conditions were confined to a specific location and a limited range of ambient temperatures and solar irradiance levels. The analysis did not encompass seasonal variations, and the system configuration was constrained by fixed component sizes (e.g., compressor capacity). Future work should therefore focus on long-term seasonal testing under real-world climatic conditions and multi-climate validation to assess broader applicability. Developing dynamic simulation models based on the present experimental results is essential for system optimization, scaling, and the exploration of alternative control strategies. Additionally, a comprehensive techno-economic assessment is recommended to evaluate the commercial viability of the proposed system.

Acknowledgements

This study was supported by the Central Guiding Funds for Local Science and Technology Development Projects (No. 236Z4503G), Industry-University-Research Collaboration Projects of Shijiazhuang in Hebei Province (No. 241010071A) and Colleges and University in Hebei Province Science Research Fund (No. CXZX2025025).

References

[1] Sezen K, Gungor A. Comparison of solar assisted heat pump systems for heating residences: A review. Solar Energy, 2023;249:424-45.

[2] Sun X, Dai Y, Novakovic V, et al., editors. Performance comparison of direct expansion solar-assisted heat pump and conventional air source heat pump for domestic hot water. 3rd International Conference on Solar Heating and Cooling for Buildings and Industry (SHC); 2014 2015.

[3] Yu S, Hu X, Li L, et al. Does the development of renewable energy promote carbon reduction? Evidence from Chinese provinces. Journal of Environmental Management, 2020;268:110634.

[4] Kong X, Zhang M, Yang Y, et al. Comparative experimental analysis of direct-expansion solar-assisted heat pump water heaters using R134a and R290. Solar Energy, 2020;203:187-96.

[5] Chen H, Wang Y, Li J, et al. Experimental research on a solar air-source heat pump system with phase change energy storage. Energy and Buildings, 2020;228:110451.

[6] Moreno-Rodríguez A, González-Gil A, Izquierdo M, et al. Theoretical model and experimental validation of a direct-expansion solar assisted heat pump for domestic hot water applications. Energy, 2012;45(1):704-15.

[7] Omojaro P, Breitkopf C. Direct expansion solar assisted heat pumps: A review of applications and recent research. Renewable and Sustainable Energy Reviews, 2013;22:33-45.

[8] Ji W, Cai J, Ji J, et al. Experimental study of a direct expansion solar-assisted heat pump (DX-SAHP) with finned-tube evaporator and comparison with conventional DX-SAHP. Energy and Buildings, 2020;207:109632.

[9] Mohamed E, Riffat S, Omer S. Low-temperature solar-plate-assisted heat pump: A developed design for domestic applications in cold climate. International Journal of Refrigeration, 2017;81:134-50.

[10] Yu X, Guo Z, Gao Z, et al. Thermodynamic investigation of a direct-expansion solar assisted heat pump with evacuated tube collector-evaporator. Renewable Energy, 2023;206:418-27.

[11] Vahidhosseini SM, Rashidi S, Hsu S-H, et al. Integration of solar thermal collectors and heat pumps with thermal energy storage systems for building energy demand reduction: A comprehensive review. Journal of Energy Storage, 2024;95:112568.

[12] Ma J, Zhu X, Fan H, et al. Size and match of the collector-evaporator for direct-expansion solar assisted heat pumps using potential alternative refrigerants. International Journal of Refrigeration, 2025;171:253-66.